Empowering the crowd: Feasible strategies to minimize the spread of COVID-19 in high-density informal settlements

Alberto Pascual-García[(1,*)], Jordan Klein[(2)], Jennifer Villers[(3,∧)], Eduard Campillo-Funollet[(4,∧)], Chamsy Sarkis[(5)]

February 8, 2021

(1) Institute of Integrative Biology. ETH-Zürich. Zürich, Switzerland.
(2) Office of Population Research. Princeton University. Princeton, NJ, USA.
(3) Princeton Environmental Institute. Princeton University. Princeton, NJ, USA.
(4) Genome Damage and Stability Centre. University of Sussex. Brighton, United Kingdom.
(5) Pax Syriana Foundation. Valetta, Malta.
(∧) Equal contribution.
(*) correspondence: alberto.pascual@env.ethz.ch

Abstract

More than 1 billion people live in informal settlements worldwide, where precarious living conditions pose unique challenges to managing a COVID-19 outbreak. Taking Northwest Syria as a case-study, we simulated an outbreak in high-density informal Internally Displaced Persons (IDP) camps using a stochastic Susceptible-Exposed-Infectious-Recovered model. Expanding on previous studies, taking social conditions and population health/structure into account, we modeled several interventions feasible in these settings: moderate self-distancing, self-isolation of symptomatic cases, and protection of the most vulnerable in "safety zones". We considered complementary measures to these interventions that can be implemented autonomously by these communities, such as buffer zones, daily health-checks, and carers for isolated individuals, quantifying their impact on the micro-dynamics of disease transmission. All interventions significantly reduce outbreak probability and mortality. Self-distancing reduces mortality by up to 35% if contacts are reduced by 50%. A similar reduction in mortality can be achieved by providing 1 self-isolation tent per 200 people. Protecting the most vulnerable in a safety zone has synergistic effects with the other interventions and reduces mortality in the most vulnerable population. Our model predicts that a combination of all simulated interventions may reduce mortality by as much as 80% and delay an outbreak's peak by more than three months. Our results highlight the potential for non-medical interventions to mitigate the effects of the pandemic. Similar measures may be applicable to controlling COVID-19 in other informal settlements, particularly IDP camps in conflict regions, around the world.

Key questions

What is already known?

- Since the onset of the COVID-19 pandemic, many studies have provided evidence for the effectiveness of strategies such as social distancing, testing, contact tracing, case isolation, use of personal protective equipment/facemasks and improved hygiene to reduce the spread of the disease. These studies underlie the recommendations of the World Health Organisation, but their implementation is contingent on local conditions and resources.
- Mathematical modelling is the basis of many epidemiological studies and has helped inform policymakers considering COVID-19 responses around the world. Nevertheless, only a limited number of studies have applied these models to informal settlements.

What are the new findings?

- We developed a mathematical model to study the dynamics of COVID-19 in Syrian IDP camps, elaborating on previous efforts done in similar settings by explicitly parametrizing the camps' demographics, living conditions and micro-dynamics of interpersonal contacts in our modelization.
- We designed interventions such as self-distancing, self-isolation and the creation of safety zones to protect the most vulnerable members of the population, among others, through conversations with camp managers with on-the-ground knowledge of what interventions would be feasible and have community buy-in.
- Our results show how low-cost, feasible, community-led non-medical interventions can significantly mitigate the impact of COVID-19 in Northwest Syrian IDP camps.

What do the new findings imply?

- Our model represents a step forward in the much-needed search for epidemiological models that are sufficiently flexible to consider specific social questions. The model can also help inform similar interventions in refugee camps in conflict-torn regions, and potentially be adapted to other informal settlements and vulnerable communities around the world.

Introduction

The COVID-19 pandemic is intensifying in regions immersed in protracted armed conflicts [**?**], where large portions of their populations have become displaced. When the displaced population exceeds official resettlement and refugee camp capacity, Internally Displaced Persons (IDPs) must live in informal settlements (hereafter named "camps"). These regions must contend with the public health challenges resulting from violence [**?**], the deterioration of health-systems [**?**], especially of critical care [**?**], and the breakdown of essential public infrastructure such as water and sanitation systems [**?**]. Urgent action is needed to contain the virus in these settings, a task which necessarily involves the engagement of the communities living in them [**?**].

This study focuses on the Northwest region of Syria (NWS): a relatively small geographical area with 4.2 million people, of which 1.15 million (27.4%) are IDPs living in camps [**?**], and where the number of cases increased twenty-fold between September 8th and October 20th, 2020 [**?**]. The health status of households in camps in NWS is poor; 24% have a member with a chronic disease, of whom 41% have no access to medicines [**?**]. As in other conflict regions, the political instability in NWS hinders coordinated public health actions, and the ongoing movements of IDPs create ample opportunity for infectious disease transmission, while making contact tracing interventions infeasible.

To investigate feasible COVID-19 prevention interventions in the camps, we considered a Susceptible-Exposed-Infectious-Recovered model similar to the one presented in [**?**], in which the camps' populations are divided into classes reflecting their estimated age-structures and comorbidity prevalence. We use this model to propose various interventions aimed at reducing the number of contacts within and between population classes in general, and with symptomatic individuals in particular. We paid special attention to how the living conditions in informal camps inform the assumptions underlying our proposed interventions, a question often neglected [**?**]. We modeled interventions previously proposed for African cities [**?**], such as self-distancing, isolation of symptomatic individuals and the creation of a 'safety zone' in which more vulnerable members of the population are protected from exposure to the virus.

Building upon the approach used to model the impact of these interventions in African cities, our model includes a parameterization of the contacts each individual has per day [**?**]. We further elaborate upon this approach by making a more explicit representation of contacts and other parameters in the model. We consider the micro-dynamics of contacts, the time that individuals take to recognize their symptoms before self-isolating, the effect of having carers to attend to isolated individuals, and the existence of a buffer zone in which exposed and protected population classes can interact under certain rules. We examine a potential worst-case scenario in which there is no access to any healthcare facility. Since empowering local communities in conflict regions to understand how to control COVID-19 is possibly the most (and perhaps only) effective way to minimize its spread, our models are of utmost importance for informing the implementation of realistic interventions in these regions.

Methods

The model

We consider a model simulating a viral outbreak in a single camp over a 12-month period inspired by those proposed by [**?**] [**?**] (see Fig. 1). The model is adapted to the context of NWS IDP camps and is divided into compartments containing individuals at different possible stages along the disease's progression, governed by the following set of differential equations:

$$\dot{S}_i = -\lambda_i S_i \tag{1}$$
$$\dot{E}_i = \lambda_i S_i - \delta_{\mathrm{E}} E_i \tag{2}$$
$$\dot{P}_i = \delta_{\mathrm{E}} E_i - \delta_{\mathrm{P}} P_i \tag{3}$$
$$\dot{A}_i = (1-f)\delta_{\mathrm{P}} P_i - \gamma_{\mathrm{A}} A_i \tag{4}$$
$$\dot{I}_i = f\delta_{\mathrm{P}} P_i - (l_i\gamma_I + h_i\eta + g_i\alpha) I_i \tag{5}$$
$$\dot{H}_i = h_i\eta I_i - \gamma_{\mathrm{H}} H_i \tag{6}$$
$$\dot{R}_i = \gamma_{\mathrm{A}} A_i + l_i\gamma_{\mathrm{I}} I_i + (1-\sigma)\gamma_{\mathrm{H}} H_i \tag{7}$$
$$\dot{D}_i = g_i\alpha I_i + \sigma\gamma_{\mathrm{H}} H_i \tag{8}$$

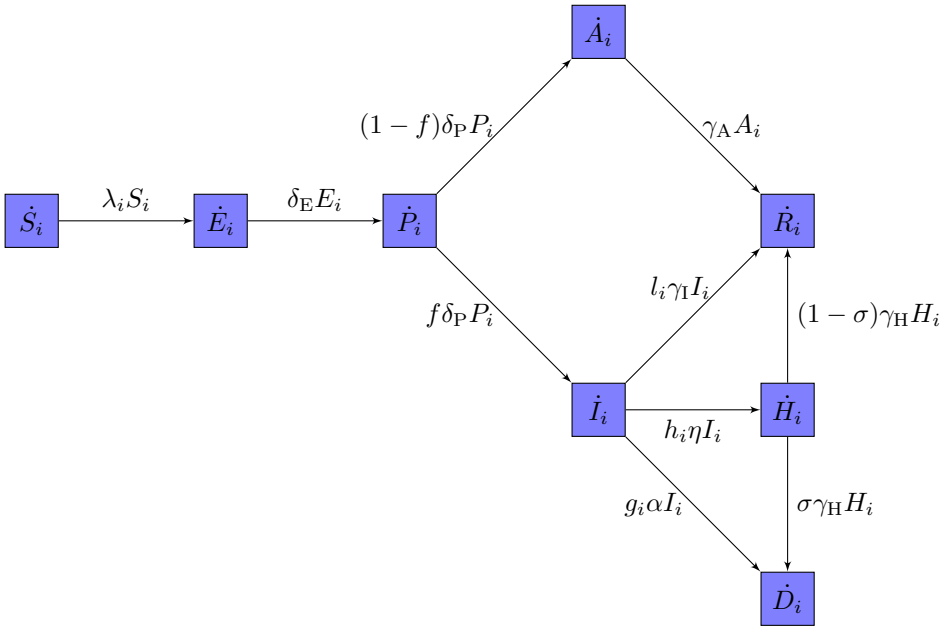

Figure 1: **Diagram of the model.** The model considers the following compartments: susceptible (S), exposed (E), infectious-presymptomatic (P), infectious-asymptomatic (A), infectious-symptomatic (I), infectious-requiring hospitalization (H), recovered (R) and dead (D).

The susceptible population (S_i) becomes exposed at rate λ_i, while exposed individuals (E_i) progress through the latent period at rate δ_{E} to a preclinical infectious stage (P_i), which then progresses to (at rate δ_{P}) either a a clinical (symptomatic, I_i, with probablity f) or subclinical (asymptomatic, A_i, with probability $1-f$) infectious stage. Asymptomatic cases recover (R_i) at rate γ_{A}. Symptomatic cases have 3 potential outcomes: mild cases will recover at rate γ_{I}, severe cases will progress to an extended infectious period during which they require hospitalization (H_i) at rate η, while critical cases requiring ICU care will die (D_i) at rate α. Finally, since the fate of individuals in the hospitalized compartment is uncertain if healthcare is not available, we run simulations considering two possibilities: either all recover ($\sigma = 0$), or all die ($\sigma = 1$) (see Table 1).

The model splits the population into classes (indexed i) to account for heterogeneity with respect to clinical risk and behaviour. Working with population classes allows us to encode behavioural assumptions in the model and strike an appropriate balance between generality, computational tractability, and the requisite specificity to realistically evaluate our proposed interventions [**?**]. Moreover, the explicit representation of contacts between and within population classes allows us to design interventions considering cultural and context-specific assumptions [**?**] (see section Interventions and Supplementary Material for details). Under a null model where no interventions are implemented, the distinctions between classes are only dependent on age and comorbidity status (hereafter "demographic-classes"). h_i, g_i and l_i are demographic-class specific parameters, adjusted to ensure that the

proportions of symptomatic cases progressing through each of the 3 potential clinical outcomes (mild, severe, and critical) are consistent with the literature (see section Epidemiological severity assumptions).

Under some interventions, the demographic-classes may be subdivided further into subclasses according to behaviour ("behaviour-classes"). Consequently, different interventions may require models with different numbers of classes. We refer to both demographic- and behaviour-classes generically as "classes" (see section Interventions for the modelization of behaviour-classes).

Table 1: **Fixed parameters.**

Parameter	Description	Value	Distribution	Reference
$1/\delta_E + 1/\delta_P$	Incubation period (days)	5.2 (95% CI: 4.1-7.0)	Lognormal	[?]
$1/\delta_P$	Presymptomatic infectious period (days)	2.3 (95% CI: 0.8-3.8)	Gaussian	[?, ?]
$1/\delta_E$	Latent period (days)	$(1/\delta_E + 1/\delta_P) - 1/\delta_P$ (Minimum = .5 days)		Derived
$1/\gamma_I$	Symptomatic infectious period (days)	7	---	[?, ?]
$1/\gamma_A$	Asymptomatic infectious period (days)	7	---	[?, ?]
$1/\eta$	Time from symptom onset to requiring hospitalization (days)	7 (IQR: 4-8)	Gamma	[?]
$1/\alpha$	Time from symptom onset to death (critical cases, days)	10 (IQR: 6-12)	Gamma	[?]
$1/\gamma_H$	Time from requiring hospitalization to recovery/death (days)	10 (IQR: 7-14)	Gamma	[?]
f	Probability an infectious individual is symptomatic	0.84 (95% CI: 0.8-0.88)	Binomial	[?]
σ	Indicator of whether hospitalized recover or die	$\sigma \in \{0, 1\}$	---	Assumed

(See Supplementary Material for derivations.)

Transmissibility assumptions

Although individuals in IDP camps share tents with other co-occupants, whom they may be more likely to infect than occupants of different tents, we ignore spatial structure in our model and assume a well-mixed population. This is justified since our following derivation of the transmissivity parameter itself, τ, is not spatially explicit.

The rate at which susceptible individuals become exposed is

$$\lambda_i = \sum_{j=1}^{n} \tau C_{ij} \frac{\beta_P P_j + \beta_A A_j + \beta_I I_j + \beta_H H_j}{N_j}, \tag{9}$$

where C_{ij} is the average number of contacts that individuals of class i have with individuals of class j per day and N_j is the total population size of class j. We parametrized C_{ij} by multiplying the mean number of total contacts that individuals from a population class i have per day, c_i, by the probability of random interaction with individuals of class j. Considering a well-mixed population, this probability is proportional to class j's fraction of the total population, i.e. $C_{ij} = c_i N_j / N$. If interventions are absent, we consider demographic-classes only and, hence, different values of c_i reflect heterogeneity in the number of contacts by age group. We assume specific values of c_i for each class baed on conversations with camp managers in NWS (see Table 3).

The probability of infection if there is a contact between a susceptible and an infected person is $\tau\beta_{\mathrm{P}}$, $\tau\beta_{\mathrm{A}}$, $\tau\beta_{\mathrm{I}}$ or $\tau\beta_{\mathrm{H}}$ depending upon whether the infected individual is in the presymptomatic (P_i), symptomatic (I_i), asymptomatic (A_i), or hospitalized compartment (H_i), respectively. The τ parameter is the maximum transmissivity, which is observed at the presymptomatic stage [**?**]. Thus, we selected the presymptomatic stage as a reference ($\beta_P = 1$) with the remaining β parameters set relative to β_{P} ($\beta_i < \beta_{\mathrm{P}}, \quad i \in \{\mathrm{A}, \mathrm{H}, \mathrm{I}\}$) based on the following set of equations (see Table 2, Supplementary Materials for derivation):

$$\beta_{\mathrm{I}} = \frac{\beta_{\mathrm{P}}\gamma_{\mathrm{I}}\gamma_{\mathrm{H}}(1 - AUC_P)}{AUC_P\delta_{\mathrm{P}}(\gamma_{\mathrm{H}} + \rho_{HI}\gamma_{\mathrm{I}})} \tag{10}$$

$$\beta_{\mathrm{A}} = \frac{\rho_{AI}\beta_{\mathrm{P}}\gamma_{\mathrm{I}}\gamma_{\mathrm{H}}(1 - AUC_P)}{AUC_P\delta_{\mathrm{P}}(\gamma_{\mathrm{H}} + \rho_{HI}\gamma_{\mathrm{I}})} \tag{11}$$

$$\beta_{\mathrm{H}} = \frac{\rho_{HI}\beta_{\mathrm{P}}\gamma_{\mathrm{I}}\gamma_{\mathrm{H}}(1 - AUC_P)}{AUC_P\delta_{\mathrm{P}}(\gamma_{\mathrm{H}} + \rho_{HI}\gamma_{\mathrm{I}})} \tag{12}$$

Table 2: **Transmissibility parameters.**

Parameter	Description	Value	Distribution	Reference
AUC_P	Presymptomatic area under infectivity curve	.44 (95% CI: .30-.57)	Gaussian	[**?**]
ρ_{AI}	Ratio of asymptomatic to symptomatic infectiousness	.58 (95% CI: .34-.99)	Lognormal	[**?**]
ρ_{HI}	Ratio of hospitalized to symptomatic infectiousness	.48	-	[**?**]

The τ parameter was estimated by randomly generating a value for the basic reproduction number, R_0, following a Gaussian distribution with a mean of 4 (99% CI: 3–5) and dividing this value by the the dominant eigenvalue of the Next Generation Matrix (see section Computational implementation for details and Supplementary Material for the analytical results). The distribution of R_0 was a compromise between values reported in the literature from regions with high-density informal settlements: R_0=2.77 in Abuja and 3.44 in Lagos, Nigeria [**?**], 3.3 in Buenos Aires [**?**], and 5 in Rohingya refugee camps in Bangladesh [**?**].

Population structure of demographic-classes

We parameterized the model with data from IDPs in NWS [**?**]. The population sizes of informal camps are approximately log-normally distributed, with a mean of of 1212. We simulated camps with populations of 500, 1000 and 2000 individuals. Since interventions tend to be less effective in larger camps, the results presented refer to simulations with 2000 individuals, unless otherwise specified. For our demographic-classes, we considered 3 age groups: children (age 1, 0-12 years old), younger adults (age 2, 13-50 yrs) and older adults (age 3, >50 yrs). For ages 2 and 3, we considered two subclasses comprising healthy individuals and individuals with comorbidities (see Table 3).

We estimated the fractions of symptomatic cases in each demographic-class that would become severe (q_i^H) and critical (q_i^D) using data from developed countries with superior population health [**?**, **?**] (see Table 3). Following previous work [**?**], we mapped the age-specific case severity distributions of the NW Syrian adult population to those of 10 years older age groups in developed countries.

Table 3: **Demographic class-specific parameters.**

		Demographic-class					
Parameter	Description	Age 1 (0-12)	Age 2 (13-50), no comorbidities	Age 2 (13-50), comorbidities	Age 3 (>50), no comorbidities	Age 3 (>50), comorbidities	References
Fraction in class	-	.407	.471	.0626	.022	.0373	[**?**, **?**]
c_i	Mean contacts per day	25	15	15	10	10	From camp managers
q_i^H	Fraction of symptomatic cases severe	.064	.067	.199	.183	.445	[**?**, **?**]
q_i^D	Fraction of symptomatic cases critical	.0065	.02	.094	.063	.222	[**?**, **?**]

(See Supplementary Material for derivations.)

Epidemiological severity assumptions

In NWS, there are 4 active and 2 planed COVID-19 referral hospitals, with a current capacity of 66 ventilators, 74 ICU beds and 355 ward beds for 4.2 million people [**?**, **?**]. Estimations based on an exponential growth model from Hariri et al. predicted a collapse of health facilities 8 weeks into an outbreak [**?**]. Although we do not have access to official data on healthcare occupancy, the currently reported number of cases suggests that this scenario could already have been reached [**?**]. Hence, we considered a worst-case scenario in which individuals will not have access to healthcare and assumed that all critical cases (those requiring ICU care) would die. However, there is greater uncertainty about the fate of severe cases, those requiring hospitalization but not ICU care. We therefore considered a compartment for severe cases to account for a longer infectious period if they stay in the camp (see compartment H_i, Fig. 1). This compartment also helped us model some interventions more realistically, for example by noting that the symptoms of severe cases are incompatible with self-isolation. To estimate upper and lower bounds for the outcome variables of our model, we simulated two possible scenarios for the fate of this compartment: one in which all cases recover, and another in which all die. In the simulations presented in the Main Text, we consider the worst-case scenario in which all of these cases die.

The fractions of symptomatic cases that are severe (q_i^{H}), critical (q_i^{D}) and recover (q_i^{R}, where $q_i^{\mathrm{R}} = 1 - q_i^{\mathrm{H}} - q_i^{\mathrm{D}}$) are demographic-class-specific (see Table 3). Since the rates at which clinical symptomatic individuals (I_i) resolve into these three epidemiological outcomes is different (η for H, α for D and γ_{I} for R) we introduced three parameters, h_i, g_i and l_i, to distribute individuals according to the desired proportions:

$$q_i^{\mathrm{H}} = h_i \eta z^{-1} \tag{13}$$

$$q_i^{\mathrm{D}} = g_i \alpha z^{-1} \tag{14}$$

$$q_i^{\mathrm{R}} = 1 - q_i^{\mathrm{H}} - q_i^{\mathrm{D}} = l_i \gamma_{\mathrm{I}} z^{-1}, \tag{15}$$

where $z = h_i\eta + g_i\alpha + l_i\gamma_{\mathrm{I}}$. The solution ... XXX in Suppl. Material.

Computational implementation

We considered a continuos-time Markov process with discrete variables, in which individuals jump from one epidemiological compartment to another with instant transition rates determined by Eqs. 1–8. The specific values of the parameters shown in these equations and of R_0 are independently drawn at each integration step from the probability distributions shown in Tables 1, 2 and 3. The Next Generation Matrix is also computed at each integration step from the parameters drawn, and τ is then estimated. To ensure computational efficiency, all these random values are precalculated. In the code provided it is possible to fix the seed to exactly reproduce the results presented. The equations are then integrated with a Gillespie algorithm implented in the adaptivetau package [Ref] in R [**?**]. Our simulations start with a completely susceptible population where one person in the

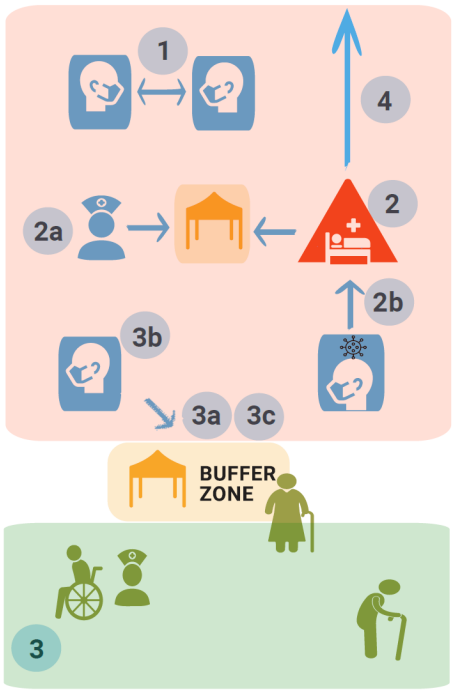

	Intervention/Description	Levels/Effect
1	**Self-distancing:** reduction of mean number of contacts per day per individual	20%, 50%
2	**Self-isolation** Isolation of symptomatic people in individual tents	Number of available tents: 10, 20, 50, 100, 250, 500, 1000, 2000
2a	Number of carers: number of healthy people that will take care of self-isolated people	1 per tent
2b	Self-isolation delay: time from symptom onset to self-isolation	12h, 24h, 48h
3	**Safety zone** Designated area for vulnerable population	Older adults only, Older adults + adults with comorbidities, Older adults + adults with comorbidities + healthy adults and kids, up to 20%, 25%, or 30% of the population
3a	Number of contacts people in the safety zone can have with people from the exposed zone (contacts always happen in the buffer zone)	2 or 10 contacts per week per individual residing in the safety zone
3b	Health checks	Exclude symptomatic people from meeting with people from the safety zone
3c	Lockdown of safety zone if one case is detected in the exposed zone	Reduces value of 3a by 50%, or 90%
4	**Evacuation of severely symptomatic**	Evacuated individuals cannot infect other people from the camp, but they do not receive healthcare
	Buffer zones Open space, 2m distancing, use of face cover	Reduces probability of infection by 80%

Figure 2: **Diagram of interventions.**

younger adult population is exposed to the virus. We verified that a steady state was always reached before the end of each simulation. We did not consider migration, births, nor deaths due to other causes, since they are small enough in magnitude to not significantly impact the course of an outbreak, provided additional conflict does not erupt.

Interventions

We considered as a null model (indexed with superscript 0) a well-mixed population in which, if there are no interventions, the average number of contacts that individuals of class i have in a camp per day is c_i (see Table 3), and hence the null contacts matrix is:

$$C^0_{ij} = c_i N_j / N, \tag{16}$$

Some of the interventions we considered either reduce the average number of contacts of each class (e.g. self-distancing) by a factor ζ or adjust the probability that individuals of class i interact with those of class j (e.g. safety zone strategies), by a factor m_{ij}. The contact matrix resulting from management strategies can therefore be written with respect to the null model as:

$$C_{ij} = (1-\zeta) m_{ij} c_i N_j / N = (1-\zeta) m_{ij} C^0_{ij} = M_{ij} C^0_{ij}. \tag{17}$$

We name the matrix M_{ij} the management matrix. In addition, in some specific interventions, we envisioned the existence of zones (called buffer zones); open spaces, with guidelines in place to limit occupancy to 4 individuals wearing masks, with 2 meters separating individuals, reducing transmissivity by 80%, denoted $\xi = 0.2$.

Self-distancing

The first non-medical intervention that we modeled is a reduction in the mean number of contacts per individual per day for the whole camp population (see Fig. 2-1). Each individual's contact rate c_i (see Table 3) was reduced by $\zeta \in \{.1, .2, .3, .4, .5\}$. Since the mean number of inhabitants per tent in a camp is 5.5 and sanitation facilities are shared [**?**], we inferred that the number of contacts per day cannot be reduced by more than 50%. For a younger adult, this would mean 7.5 contacts per day.

Self-isolation

Self-isolation is a challenge in informal settlements, where households consist of a single (often small) space, water is collected at designated locations, sanitation facilities are communal and food supplies are scarce. We considered the possibility of those showing symptoms self-isolating in individual tents in dedicated parts of the camps. We simulated this intervention with various numbers of isolation tents per camp, ranging from 10 to 2000 for a camp of 2000 people (see Fig. 2-2). In addition, we modeled the role of carers dedicated to providing for isolated individuals (see Fig. 2-2a), making the following assumptions. We considered a number N_{care} of carers having c_{care} contacts per day with the isolated population. Carers are entirely drawn from younger adults with no comorbidities, and must have no symptoms. We denote the number of individuals fulfilling these requirements with N_{exp} (number of exposed). When the number of symptomatic individuals exceeds the isolation capacity, $\tilde{N}$, the individuals in excess are fully infectious (note that we use a tilde to denote variables related to the isolated population). In addition, the occupancy of the isolation beds is distributed among classes proportionally to the number of symptomatic individuals present in each class, i.e. $\tilde{I}_j = \tilde{N}\left(I_j / \sum_j I_j\right)$. Finally, symptomatic individuals that would require hospitalization become fully infectious. We make this assumption since camps lack the necessary means to adequately protect the rest of the population when individuals require more dedicated care; it is unlikely that a severely ill individual would be able to stay alone in a tent.

Given these assumptions, to estimate the rate of exposure for each demographic-class, we split our expression of contacts into two terms, one describing the interaction of individuals in the class with the isolated population, and another for interaction with infectious individuals who are not isolated:

$$\lambda_i = \tau \sum_j \underbrace{\beta_{\text{I}} \tilde{c}_i \tilde{P}(i \to j)}_{\text{isolated}} + \underbrace{C_{ij} \frac{\beta_{\text{P}} P + \beta_{\text{A}} A_j + \beta_{\text{I}} \Theta(N_{\text{I}} - \tilde{N})(I_j - \tilde{I}_j) + \beta_{\text{H}} H_j}{N_j}}_{\text{not isolated}}, \tag{18}$$

where $\tilde{c}_i$ is the mean number of contacts of class i per individual per day with the self-isolated individuals and $\tilde{P}(i \to j)$ is the probability that an individual of class i encounters an isolated individual of class j. For the not-isolated term, we maintain the well-mixed population assumption with the incorporation of a Heaviside function, $\Theta(N_{\text{I}} - \tilde{N})$, which activates the interaction with the clinical symptomatic individuals when their number N_{I} exceeds the isolation capacity $\tilde{N}$, and we estimate the probability of interacting with non-isolated individuals to be proportional to their fraction $(I_j - \tilde{I}_j)/N_j$. For the isolated population, however, the well-mixed assumption is no longer valid. Firstly, all demographic-classes not contributing to the group of carers will never interact with the isolated individuals, and hence $\tilde{c}_i = 0$ for them (morever $\tilde{P}(i \to j) = 0$). Secondly, the healthy younger adults population will certainly interact with isolated individuals through their role as carers, hence $\tilde{P}(i \to j) = 1$.

To estimate $\tilde{c}_i$ for the healthy younger adult class, we note that the number of contacts per day with the isolated individuals is $c_{\text{care}} N_{\text{care}}$, and hence the mean number of contacts per individual per day is $\tilde{c}_i = c_{\text{care}} N_{\text{care}} / N_{\text{exp}}$. We observe that, increasing the number of carers, and the number of contacts per day between carers and individuals, will increase the rate of infection. For simplicity, we assume that there is one carer for each infected person in the class j, ($N_{\text{care},j} = \tilde{N}_j$), having only one contact per day (c_{care}). Note the convenience of this choice, since if the number of symptomatic individuals is larger than the number of potential carers, the ratio $\tilde{N}_j / N_{\text{exp}} > 1$, implying more than one contact per day is needed to take care of that population class. We assume that contacts between carers and isolated individuals take place in a buffer zone.

With these considerations, using 9 we can express the rate of exposure of the healthy younger adult demographic-class (indexed k) as:

$$\lambda_k = \tau \sum_j \xi \frac{\tilde{N}_j}{N_{\text{exp}}} + C_{kj} \frac{\beta_{\text{P}} P + \beta_{\text{A}} A_j + \beta_{\text{I}} \Theta(N_{\text{I}} - \tilde{N})(I_j - \tilde{I}_j) + \beta_{\text{H}} H_j}{}, \tag{19}$$

For the remaining classes ($i \neq k$) the rate of infection (9) becomes:

$$\lambda_i = \tau \sum_j C_{ij} \frac{\beta_{\text{P}} P + \beta_{\text{A}} A_j + \beta_{\text{I}} \Theta(N_{\text{I}} - \tilde{N})(I_j - \tilde{I}_j) + \beta_{\text{H}} H_j}{}. \tag{20}$$

We also considered minimum time intervals for individuals to recognize their symptoms and self-isolate (see Fig. 2-2b). To model this, whenever simulating the isolation intervention, the symptomatic compartment is split in two: symptomatic prior to identification, O_i, and symptomatic following identification, I_i. We assumed the

duration of O_i follows a Gaussian distribution with means 12, 24 or 48 hours on average. The duration for which an individual isolates is then calculated as the difference between the symptomatic period if there is no isolation and the duration spent in the symptom onset compartment.

Safety zone

In this intervention, the camp is divided in two areas: a safety zone, in which a certain fraction, f_{S}, of the population, mostly those more vulnerable, live (hereby referred to as a "green" zone following previous studies [**?**], denoted g), and an exposed ("orange", o) zone with the remaining population. In our simulations, the first exposed individual always belongs to the orange zone. Implementing this intervention requires splitting some demographic-classes into two behaviour-classes. For example, if some healthy younger adults are allocated to the green zone, we split the demographic-class "healthy younger adults" into "orange" and "green" behaviour-classes, to model the different contacts that these two subclasses of healthy younger adults will have amongst themselves and with other classes. Since proposals for partitioning the population may be received differently across camps, we considered several scenarios for allocating a camp population to the two zones (see Fig. 2-3). In Supplementary Table **??** we present the classes considered in each scenario. In our simulations, we considered limiting individuals in the green zone to 10 or 2 contacts with individuals from the orange zone per week (see Fig. 2-3a). Other variations of this intervention we explored include preventing symptomatic individuals from entering the buffer zone (see Fig. 2-3b) and a "lockdown" of the green zone, where the number of weekly contacts in the buffer zone is reduced by 50% or 90% (see Fig. 2-3c).

Each individual in the green zone can interact with a limited number (c_{visit}) of family members (hereafter "visitors") from the orange zone per day exclusively via a buffer zone (see previous section), but the living conditions within both zones remain the same, so the overall contact rate does not change unless self-distancing is also implemented. Although we do not expect this assumption to be true in general, it allows us to investigate undesired side-effects of this intervention, such as older adults having increased contact amongst themselves if isolated together. Since the number of contacts between the green zone and the orange zone are reduced but the overall mean daily contacts, c_i, are conserved, we need to estimate how contacts will be redistributed from individuals from a different zone to individuals living in the same zone. Since interaction is limited to others in the same zone, we also need to account for individuals having a higher likelihood of interaction with members of the classes staying in the same zone compared to the null model. The safety zone interventions are thus governed by the parameter m_{ij}, a matrix which modifies the probability that an individual in class i has a potentially infectious contact with an individual in class j:

$$m_{ij} = \frac{\xi N \rho c_{\mathrm{visit}}}{c_i N_{\mathrm{Y}}} \quad (i,j \text{ in different zones i}\in\mathrm{X} \text{ and j}\in\mathrm{Y}) \tag{21}$$

$$m_{ij} = \frac{N(1-\rho c_{\mathrm{visit}})}{c_i N_{\mathrm{X}}} \quad (i,j \text{ in same zone } X). \tag{22}$$

Where N is the total number of individuals in the camp, N_{X} the total number of individuals in the same zone $X \in \{\mathrm{o},\mathrm{g}\}$ and N_{Y} the total number of individuals in the other zone $Y \in \{\mathrm{o},\mathrm{g}\}$. If we assume that visitors are always different, the quantity $f_{\mathrm{o,visit}} = c_{\mathrm{visit}} \frac{N_{\mathrm{g}}}{N_{\mathrm{o}}}$ is the fraction of the orange population that visits the buffer zone. We define ρ as:

$$\rho = \begin{cases} 1 & \text{if } i \in \mathrm{g} \\ f_{\mathrm{o,visit}} & \text{if } i \in \mathrm{o} \end{cases} \tag{23}$$

(See Supplementary Materials for derivations.)

In some interventions we considered that individuals visiting the buffer zone will have a health check (e.g. temperature measurement), aimed at excluding symptomatic individuals. When the health check is applied, the transmission probability between individuals from the orange zone in the I or H compartments and individuals from the green zone is set to zero.

Evacuation

The last intervention we simulated is the evacuation of severe cases (individuals in the hospitalization compartment). Since they require more intensive care that cannot be delivered while adhering to the guidelines of a buffer zone, severe cases were assumed to be fully infectious and not able to self-isolate. Once severe cases are evacuated,

their infectivity is reduced to zero (see Fig. 2-4). The fate of severe cases is not altered by this intervention since we assumed that hospitals are saturated and that evacuees are transferred to isolation centers instead. We model evacuation considering a parameter $\epsilon = 0$ if evacuation is put in place and $\epsilon = 1$ otherwise. Thus, equation 9 (without considering the other interventions) becomes:

$$\lambda_i = \sum_{j=1}^{n} \tau C_{ij} \frac{\beta_{\mathrm{P}} P_j + \beta_{\mathrm{A}} A_j + \beta_{\mathrm{I}} I_j + \epsilon \beta_{\mathrm{H}} H_j}{N_j} \tag{24}$$

Statistical analysis

For each implementation of the interventions, we ran 500 simulations and compared results between them. The main variables considered are the fraction of simulations in which at least one death is observed, a proxy for the probability of an outbreak, the fraction of the population that dies and the time until the symptomatic population peaks, as well as the infection fatality rate (IFR) and fraction of the population that recovers. For consistency, we only considered simulations in which there was an outbreak when comparing the outcome of a variable between interventions. We used the Shapiro-Wilk test [**?**] to verify that our results do not exhibit normally distributed residuals, Kruskal-Wallis test for pairwise comparisons [**?**], and Conover-Iman test for multiple comparisons [**?**]. The model and all statistical analyses were implemented in R; we used the package PMCMRplus [**?**].

Results

In the absence of interventions, the mean IFR is ∼2% in simulations where all severe cases requiring hospitalization recover (see Supplementary Fig. **??**), and ∼11% in simulations where all severe cases die. We consider the latter scenario to evaluate the effect of non-medical preventive interventions. In this scenario, the probability of observing an outbreak is close to 0.85, in which ∼10% of the camp dies, the number of symptomatic cases peaks after 55 days and ∼84% of the population recovers.

Self-distancing

Our results show that self-distancing has a notable effect on reducing the probability of an outbreak: a 20% reduction in daily contacts is associated with a ∼10% decrease in outbreak probability (see Fig. 3A). A greater reduction in daily contacts, of 50%, is required to observe a significant decrease in mortality, of as much as 35% (see Fig. 3B). Self-distancing also significantly extends the time until the peak of the outbreak, from 55 days when there is no intervention to 110 days when contacts are reduced by 50% (see Fig. 3C). However, the proportion of the population recovered after 12 months is reduced by ∼30% (see Supplementary Fig. **??**).

Self-isolation

With only 10 tents for a camp of 2000 people (i.e. 1 tent for every 200 people), self-isolation yields a modest decrease in the probability of observing an outbreak (see Fig. 3D), but a stronger reduction in mortality (∼30%) (see Fig. 3E). Further increasing the number of tents significantly augments this reduction until there is 1 per every 20 people (Kruskal-Conover post-hoc-test, p-val$< 3 \times 10^{-5}$). However, mortality begins to slightly increase again after this threshold. This effect and the increase in the probability of observing an outbreak are consequences of having one carer per individual isolated (see Supplementary Material), so when the isolated (infected) population increases, the number of healthy younger adults in contact with them increases in tandem. Similarly, we observe a reduction in IFR when increasing the number of tents up to 1 per every 20 people, and no significant reduction over that number (see Supplementary Fig. **??**). Importantly, the potential reductions in overall fatalities and IFR from self-isolation are realized whether the time required for individuals to recognize their symptoms is 12h or 24h on average, but the intervention becomes less effective when this time increases to 48h (see Supplementary Fig. **??**).

Safety zone

In this section, we consider the scenario in which all older adults, younger adults with comorbidities and their family members up to 20% of the camp population live in the green zone, unless otherwise specified. Creating

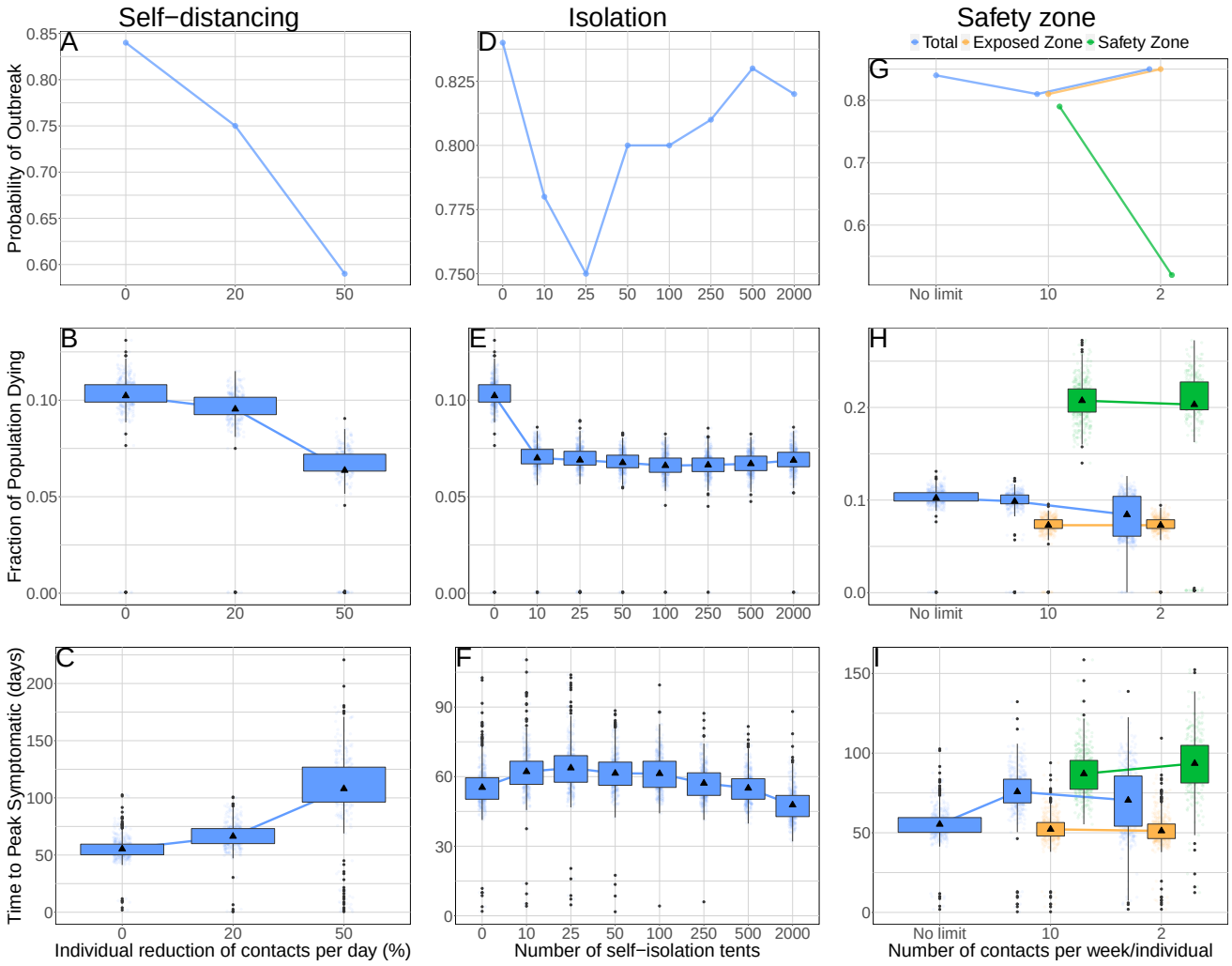

Figure 3: **Effect of interventions on outbreak probability, fatalities and time until symptomatic cases peak.** A: Self-distancing, probability of an outbreak. B: Self-distancing, fraction of the population dying. C: Self-distancing, time until peak symptomatic cases. D: Self-isolation, probability of an outbreak. E: Self-isolation, fraction of the population dying. F: Self-isolation, time until peak symptomatic cases. G: Safety zone, probability of an outbreak. H: Safety zone, fraction of the population dying. I: Safety zone, time until peak symptomatic cases. Note that in figures of the safety zone intervention (panels G-I), the mean of an outcome for the whole population is not the weighted mean of the exposed and safety zones, since outcomes are computed considering simulations in which at least one death was observed in the population class inhabiting the zone. This explains why in panel I there is a reduction in the mean time until symptomatic cases peak when moving from 10 to 2 contacts per week for the whole population, despite there being an increase in the safety zone: in ∼35% of simulations there is an outbreak in the orange zone but not in the green zone (panel G).

a green zone improves the effect of the previous interventions overall, but with sometimes opposite outcomes in the exposed and protected populations. For example, the probability of an outbreak sharply decreases for the protected population, by almost 40%, if only two contacts are allowed per week in the buffer zone (see Fig. 3G). Notably, most of this reduction is only achieved when health-checks excluding symptomatic individuals from the buffer zone are in place (see Supplementary Fig. **??**). On the other hand, the probability of an outbreak may slightly increase for the exposed population, a consequence of the relative increase in intra-zone contacts. Despite this side-effect, by shifting the burden of an outbreak towards the less vulnerable population in the orange zone, this intervention not only reduces fatalities among the more vulnerable population in the green zone (Kruskal-Wallis test, p-val$< 10^{-15}$; see Supplementary Fig. **??**), but also reduces the overall IFR (see Supplementary Fig. **??**) and thus the number of fatalities globally (see Fig. 3H). Another important outcome of this intervention is the notable increase in time until the number of symptomatic cases peaks for the vulnerable population (see Fig. 3I).

Considering different scenarios for allocating people to the green zone, the lowest probability of an outbreak is achieved when only older adults or at most older adults and younger adults with comorbidities move there (see Supplementary Fig. **??**). Positive effects of the green zone intervention are even more marked in camps with smaller populations, for every outcome of interest except time until symptomatic cases peak (see Supplementary Fig. **??**). The incorporation of a lockdown has the greatest effect on reducing the probability of an outbreak in the green zone, to under 0.10 when contacts in the buffer zone are reduced by 90%. While lockdowns show no positive effect on green zone fatalities in the few instances where an outbreak does reach there, they decrease IFR and overall fatalities by further concentrating outbreaks in the less vulnerable population (see Supplementary Fig. **??**).

Evacuation

We observe no significant effects when severe cases requiring hospitalization are evacuated (see Supplementary Fig. **??**). Since we considered that these individuals will not receive health care (they are evacuated to isolation centers), their fate remains the same than if staying in the camp and, hence, we expect evacuation to have an effect only in reducing the infectivity. Although these individuals spend a longer period being infectious with respect to an individual having mild symptoms ($\sim$10 days longer), the number of individuals under these conditions is only a small fraction of the total infectious population at any given time, what explains why we do not observe significant effects for this intervention.

Combined interventions

The effects of the interventions observed when we examine them individually build upon each other when multiple interventions are implemented in tandem (see Fig. 4 and Supplementary Fig. **??**). The protective effects of the safety zone intervention especially are most fully realized not when implemented on its own, but when paired with other interventions. They become so effective that outbreaks in the green zone become exceptionally rare, but so well controlled when they do happen, that the majority of outbreaks see fewer than 20 cases. This leads to an anomalous increase in IFR in some of the most effective interventions, driven by the discretization of the values it can take (Supplementary Table. **??**). When all interventions are implemented together: strict self-distancing (50% reduction in contacts), self-isolation of symptomatic cases (1 tent for every 40 people), a safety zone with 2 contacts per week in the buffer zone, health checks, a strict lockdown (90%), and evacuation of severe cases, mortality is reduced by $\sim$80%.

Discussion

In this study, we propose a number of interventions of immediate applicability to informal settlements. We focused on IDP settlements in NW Syria, taking into account the interventions' feasibility, cultural acceptance and their need for low-cost. When confronted with different possible scenarios, we generally considered the worst-cases, highlighting the interventions that are most effective in the direst conditions, but possibly resulting in an overestimate of mortality. This potential overestimation does not change the qualitative picture of the results, which is built upon comparison of relative values between the presence and absence of interventions.

Our results align with previous simulation studies of potential COVID-19 interventions in similarly densely populated, low-resource settings where informal settlements are present, such as urban areas of sub-Saharan

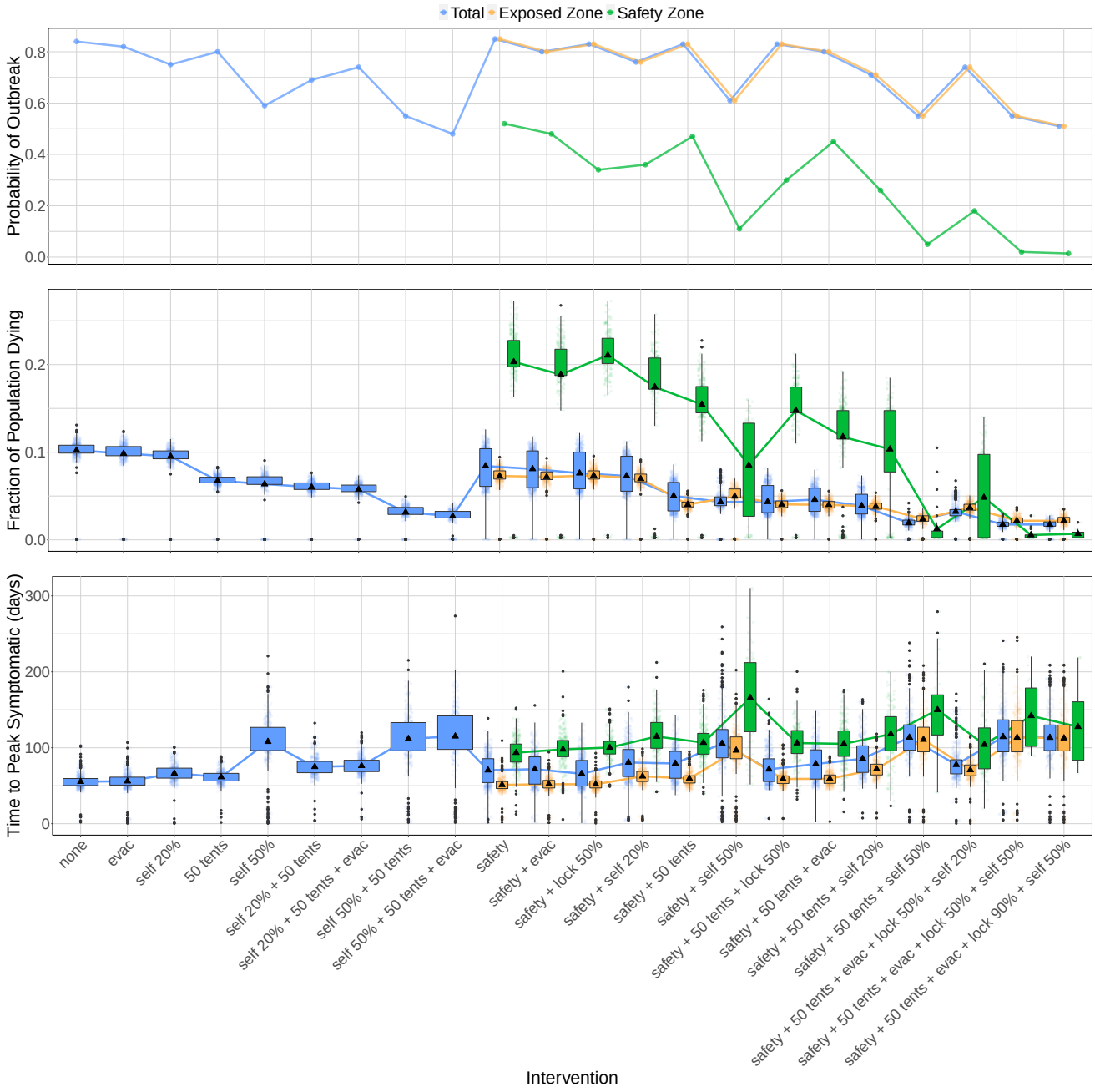

Figure 4: **Combinations of interventions.** Probability of an outbreak (top), fraction of the population dying (middle) and time until peak symptomatic cases (bottom) for different combination of interventions. Evac = evacuation of severely symptomatic, self = self-distancing, tents = number of available self-isolation tents, safety = safety zone, lock = lockdown of the buffer zone. For combinations of interventions including a safety zone, we distinguish between the population living in the green zone, in the orange zone and the whole population.

Africa. In these settings, social-distancing is demonstrated to be an effective intervention, and even small changes are estimated to have large effects on outbreaks [**?**], in some cases determining whether or not already inadequate healthcare systems become overwhelmed [**?**]. Zandvoort et al. show that similar measures to the ones we consider: self-isolation, physical distancing and "shielding" the vulnerable, may reduce mortality by 60%-75% in African cities [**?**].

Self-distancing proves to be an effective measure in our models as well; reducing contacts by 50% has the greatest effect across most outcomes of interest in any of the interventions we examined. However, the difficulty of achieving a reduction of this magnitude cannot be overlooked, especially considering the large proportion of the population composed of children, a group with an already high contact rate that may prove difficult to control [**?**].

We also propose self-isolation using individual tents which can be located in a dedicated zone or next to the tents of relatives, where contact with non-isolated individuals is mediated by a buffer zone. This intervention is effective with even a small number of isolation tents, as low as 5-10 tents per 1000 camp residents. After conversations with camp managers, we found that this intervention is more likely to be accepted in NW Syria than evacuation to community-based isolation centers. Community-based isolation not only poses cultural challenges; the capacity required to implement it has hardly been met [**?**], and it is still one of the main challenges in the region [**?**].

One of the key parameters we assessed for the implementation of self-isolation is the need for carers. In considering one carer per isolated individual, with daily contact in a buffer zone, once a certain threshold of isolated cases ($\sim$200 per camp of 2000) is surpassed, the benefits of isolation begin to be outweighed by an increase in infectivity resulting from a growing number of exposed carers. This pitfall could be circumvented through the creation of a more organized, dedicated group of carers, thus reducing the number of healthy younger adults in contact with isolated (infectious) individuals.

Much of the success or failure of the safety zone intervention hinges on the functioning of the buffer zone. The number of inter-zone contacts per week, the implementation of health checks, and potential lockdowns all have notable effects. Also important is the portion of the population that is protected; protecting only the vulnerable may have the most beneficial effects, but it is precisely these vulnerable individuals, older adults and people with comorbidities, who may most need family members to care for them. While safety zone scenarios that allow greater numbers of family members to accompany their vulnerable relatives to the green zone may confer greater epidemiological risk, they may also engender greater well-being and social cohesion.

Although setting up a safety zone sharply reduces the probability of an outbreak in the population classes with the highest IFRs, thus reducing the IFR of the entire population, it is possible that our model may overestimate mortality from an outbreak in the green zone in the few instances when there is one. Since total numbers of contacts are conserved in our modelization, individuals do not reduce their contacts when moved to the green zone, which implies an increase in the number of contacts between vulnerable individuals. Despite this increase in contacts, we observed a significant reduction in mortality in the vulnerable population when the safety zone is implemented. These results address concerns raised around this type of intervention from previous experiences with large numbers of fatalities registered in nursing-homes in developed countries [**?**]. While in developed countries nursing home residents have more contacts, both with other vulnerable people (other nursing home residents) and healthy adults who live in different households (health aids), than the elderly who live at home, vulnerable people in our proposed green zone have the same number of total contacts as they would under normal conditions, but significantly fewer contacts with healthy adults from different households.

An instrumental consideration for our models is the fraction of the population recovered from COVID-19 after a steady state is reached. Although the duration for which SARS-CoV-2 infection confers immunity is uncertain, the proportion of the population recovered after an outbreak should play a role in its protection against future ones. For every intervention except self-distancing of 50%, we observed that the fraction of the population recovered meets or exceeds 75%.

A key limitation of our approach is that it simulates an outbreak started by one infectious individual in a single camp with a closed population. We acknowledge that this approach does not fully capture the complexities of the NWS region, where IDPs live interspersed throughout the region in several hundred camps. The dynamics of an outbreak in the region are undoubtedly influenced by inter-community contacts, and the dynamics of an outbreak in a single camp by these region-wide dynamics, as it has been demonstrated in other countries [**?**, **?**]. We expect our results to be robust against changes in the population, as soon as these changes are relatively small compared to the total population size in the camp, implying punctual inputs of infected individuals. This is the expected behaviour in IDPs, which are often small and located in rural areas, and in which important

population movements, as those observed in large camps, are infrequent. This fact, together with the relatively young population in IDPs, may help in limiting the impact of the disease, as observed in African rural areas [**?**].

Other unaccounted for social and cultural dynamics will undeniably complicate the feasibility of our proposed interventions. Only one example we have not addressed here is the unlikeliness of children under 13 self-isolating. Although the number of challenges to implementing our proposed interventions are potentially endless, the community-based nature of our approach may help circumvent these challenges much faster than healthcare-based interventions, which often depend on complex political decisions and may take years to build the requisite capacity for an effective response. If the dynamics of the virus are well understood by local communities and at least some of the interventions we propose are implemented, the impacts of COVID-19 can be mitigated even in an environment as challenging as NW Syria.

Conclusion

Given a rapidly changing environment and slow responses of local and international authorities, the latter often leaving these communities aside in their priorities [**?**], empowering local communities themselves is perhaps the best, if not the only way, to help them avoid the worst consequences of the pandemic. This not only applies to IDP camps in NW Syria, but more generally to refugee camps in conflict-torn regions, and potentially other informal settlements and vulnerable communities around the world: the low-cost, effective interventions we present are feasible, needed and urgent.

Acknowledgements

This collaboration was organized by crowdfightCOVID19 (www.crowdfightcovid19.org) upon request from CS. We thank Judith Boumann for valuable contributions. We thank Peter Ashcroft, Juan Poyatos, Noreen Goldman, Burcu Tepekule and members of Sebastian Bonhoeffer's and Bryan Grenfell's groups for useful discussions. We thank two anonymous reviewers...

Declarations

Funding

ECF's research is supported by Wellcome Trust grant 204833/Z/16/Z.

Conflicts of interest/Competing interests

Alberto Pascual-García is a Board Member of crowdfightCOVID19, an initiative from the scientific community to put all available resources at service of the fight against COVID-19. Chamsy Sarkis (co-author) is a Board Member of the Pax Syriana Foundation, a non-profit organization set up for social and philanthropic purposes including promoting and providing support and assistance to civilian aid projects in the fields of education, health, emergency assistance, psychological assistance and humanitarian aid for people affected by wars or humanitarian crises. These organizations had no role in study design, data collection, data analysis, data interpretation, or writing of the article.

Ethics approval

This study used only publicly available aggregate data and was thus not subject to ethical review.

Consent to participate

NA

Consent for publication

All authors agreed on publication.

Availability of data and material

All results are available at the url https://github.com/crowdfightcovid19/req-550-Syria

Code availability

All the code is freely available at the url https://github.com/crowdfightcovid19/req-550-Syria

Authors' contributions

All authors contributed to the conceptualization. Design of the methodology: APG, ECF, JV, JK, CS. Formal analysis: APG, ECF, JK. Code development APG, ECF, JK. Conducted research: APG, ECF, JV, JK. Validate results: APG, ECF, JK, JV, CS. Contributed resources: APG, CS, ECF, JK. Data curation: APG, JK. Visualization: APG, ECF, JK. Writing (original draft) APG, ECF, JK. All authors contributed to the final version of the manuscript, and APG supervised the research.